Adaptive Large Scale Artifact Reduction in Edge-based Image Super-Resolution

Alexander Wong and William Bishop

***Abstract*— The goal of multi-frame image super-resolution is to use information from low-resolution images to construct high-resolution images. Current multi-frame image super-resolution methods are highly sensitive to prominent large scale artifacts found within the low-resolution images, leading to reduced image quality. This paper presents a novel adaptive approach to large scale artifact reduction in multi-frame image super-resolution. The proposed method adaptively selects information from the low-resolution images such that prominent large scale artifacts are rejected during the reconstruction of the high-resolution image. In addition, an efficient super-resolution algorithm based on the proposed artifact reduction method and edge-adaptive constraint relaxation is introduced. Experimental results show that the proposed super-resolution algorithm based on the proposed artifact reduction method improves the perceptual quality of the resultant high-resolution image both quantitatively and qualitatively when compared with standard super-resolution methods in situations where prominent large scale artifacts exist.**

***Index Terms*— artifact reduction, edge-adaptive, image super-resolution.**

I. Introduction

IMAGE super-resolution is the process of reconstructing high resolution (HR) images from information obtained from low resolution (LR) images. Image super-resolution methods play an important role in a wide variety of imaging and computer vision applications. Some of these applications include ultrasound image enhancement [1], [2], text enhancement for optical character recognition [3], digital video enhancement [4], [5], and remote sensing image enhancement [6], [7].

The increasing interest in producing HR images from LR images have resulted in various useful super-resolution techniques. In general, these techniques can be divided into two main groups:

1) Single-frame super-resolution, and
2) Multi-frame super-resolution.

Single-frame super-resolution techniques [6], [7], [8] utilize information from a single LR image to reconstruct a HR image. As such, the HR image does not contain any additional information compared to the original LR image and are not very beneficial for computer vision or advance image enhancement purposes. Therefore, single-frame super-resolution techniques are mainly used for general visual quality enhancement of images such as digital video upscaling. Recent research in super-resolution have focused on multi-frame super-resolution techniques, where multiple LR images are used to reconstruct HR images. Each LR image contains unique information that is not found in other LR images. By utilizing unique information from multiple LR images, it is possible to reconstruct HR images by interpolating information on a sub-pixel level. Therefore, a HR image constructed using multi-frame super-resolution techniques contain more detailed information than any of the individual LR images can provide. Such details can greatly improve the perceptual quality of an image. Furthermore, multi-frame super-resolution techniques are particularly beneficial to computer vision applications, where additional information can lead to improved performance.

A large number of multi-frame super-resolution methods have been proposed. A widely used group of multi-frame image super-resolution techniques are those based on constrained regularization. In such techniques, the super-resolution problem is formulated as a regularized optimization problem and the resultant HR image is estimated by solving the regularized optimization problem using techniques such as conjugate gradient methods [9], [10]. Another popular group of multi-frame super-resolution are those based on Projection on Convex Sets (POCS) [13], [14]. In POCS-based image super-resolution methods, an estimated HR image can be found for the super-resolution problem by projecting it onto each constraint within a convex constraint set. The constraint set is formulated such that consistency is maintained with the LR images used to reconstruct the HR image. Therefore, the estimated HR image is updated as it is projected onto constraint sets until a desired number of iterations or error condition is met. One of the drawbacks to this approach is that there is no single optimal solution. A hybrid approach that utilizes both maximum likelihood estimation and convex constraints has been proposed to address this issue [16]. A similar approach to POCS-based methods is the iterative back-projection method [15], where an initial HR image estimate is back-projected to estimate a set of LR images based on the degradation model. The error between the estimated LR images and the actual LR images is then calculated and used to refine the HR estimate. Other approaches to multi-frame super-resolution include the use of Bayesian estimation methods [11], [12], Maximum a Posteriori (MAP) estimation methods [17], and neural networks [18].

Current research in multi-frame image super-resolution methods have focused on reducing small-scale artifacts such as ringing [14], [17] and quantization noise [19]. However, research on multi-frame image super-resolution methods that focuses on large-scale artifacts such as large dirt artifacts, scratches, and large image defects have been largely ignored. Such large-scale artifacts can lead to significant loss in per-

ceptual quality in the reconstructed HR image. The goal of the proposed algorithm is to utilize both large-scale artifact reduction and an edge-based model to improve perceptual quality of the reconstructed HR image in a computationally efficient manner.

The main contribution of this paper is a novel adaptive approach to large scale artifact reduction in multi-frame image super-resolution. The proposed method adaptively selects information from the low-resolution images such that prominent large scale artifacts are rejected during the reconstruction of the high-resolution image. Furthermore, an efficient super-resolution algorithm based on the proposed artifact reduction method and edge-adaptive constraint relaxation is introduced. In this paper, a formulation of the super-resolution problem is presented in Section II. The underlying theory behind the proposed algorithm is discussed in Section III. The methods and data used to test the effectiveness of the algorithm are outlined in Section IV. Experimental results are presented and discussed in Section V. Finally, conclusions are drawn in Section VI.

II. Super-resolution Problem Formulation

The multi-frame super-resolution problem can be defined in the following manner. Suppose there exists a set of LR images $I_{\mathrm{LR},1}, I_{\mathrm{LR},2}, ..., I_{\mathrm{LR,n}}$. Each LR image can be modelled as a HR image I_{HR} degraded by various imaging conditions such as motion blur, decimation, and warping. This relationship can be written as the following expression:

$$I_{\mathrm{LR}} = HI_{\mathrm{HR}} + e \tag{1}$$

where H is the overall degradation operator, I_{HR} and I_{LR} are the HR and LR images respectively, and e is the additive noise. The overall degradation operator encompasses the overall degradation model, which may consist of multiple degradation operators. For example, a typical degradation model used for the multi-frame super-resolution problem consists of decimation and blur operators. Therefore, (1) can be written as the following expanded expression:

$$I_{\mathrm{LR}} = \left(\prod_i D_i \right) I_{\mathrm{HR}} + e \tag{2}$$

where D_i is an individual degradation operator (e.g. blur, decimation, warping, and etc.) and $H = \prod_i D_i$. Since each LR image contains unique information that is not found in other LR images, the overall degradation operator is different for each LR image. Therefore, the relationship between the HR image and the j^{th} LR images can be expressed by:

$$I_{\mathrm{LR},j} = \left(\prod_i D_{i,j} \right) I_{\mathrm{HR}} + e_j, 1 \leq j \leq n \tag{3}$$

where n is the number of LR images used to reconstruct the HR image. Based on the this relationship and known degradation operators, the super-resolution problem can be seen as an inverse problem, where the original model I_{HR} must be obtained from the observed data $I_{\mathrm{LR},1}, I_{\mathrm{LR},2}, ..., I_{\mathrm{LR,n}}$. In most real-world situations, the multi-frame super-resolution problem is generally ill-posed and result in underdetermined systems where there is no single optimal solution.

III. Theory

Prior to outlining the proposed algorithm, it is important to present the background theory behind some of the key concepts in the algorithm. First, a definition for large scale artifacts as well as the difficulties associated with such artifacts are presented. Second, the theory behind problem partitioning and how it relates to large scale artifact reduction is explained. The method used to identify and reduce the effect of large scale artifacts on the reconstructed HR image is presented. Finally, the adaptive regularized optimization method used to reconstruct the HR image is presented.

A. Large Scale Artifacts

As discussed in Section I, current research in multi-frame image super-resolution methods have focused only on reducing small-scale artifacts such as ringing [14], [17] and quantization noise [19]. Examples of some small scale artifacts are shown in Fig. 2. These are considered to be small-scale artifacts for a number of reasons. First, they generally account for a very small fraction of the overall image content. For example, ringing artifacts occur primarily around prominent edges, which make up a small portion of the actual image content. Second, the loss in perceptual quality as a result of small-scale artifacts such as ringing artifacts is generally relatively low. Finally, the general characteristics of small-scale artifacts are typically known and can be reduced in a more systematic fashion. For example, quantization noise are generally most noticeable at the block boundaries for images compressed using block transforms. Therefore, such noise can be significantly reduced systematically at the block boundaries. Similarly, ringing artifacts are localized around prominent edges and can be significantly reduced systematically by filtering at these edges.

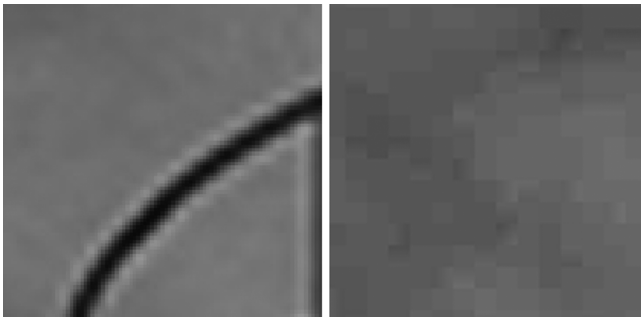

Fig. 1. Example of small scale artifacts. Left: ringing artifacts; Right: quantization noise

Large scale artifacts can be defined as artifacts that possess the following characteristics. First, large scale artifacts cover a relatively large area in a LR image. Due to such artifacts, a significant portion of the LR image may contain erroneous information that contribute to the HR image in a negative

manner. Therefore, common filtering techniques cannot be used to correct such large artifacts. Hence, large scale artifacts result in a significantly loss in perceptual quality in the reconstructed HR image. Furthermore, the general characteristics of large-scale artifacts are not known as they can vary greatly from one LR image to another. This makes it difficult to use filtering techniques based on specific characteristics or properties. Based on the above definition, some examples of artifacts that fall into the category of large scale artifacts include:

1) large dirt and dust artifacts,
2) large scratches,
3) artifacts due to camera defects or damage, and
4) objects that move in and out of frame.

Examples of large scale artifacts are shown in Fig. **??**. All large scale artifacts result in significant occlusion of information in the LR images that can be otherwise be used to reconstruct the HR image. As such, large scale artifacts can be further be generalized into two main groups: i) temporary occlusions, and ii) permanent occlusions. Temporary occlusions are artifacts that appear and disappear over a period of time. As such, a LR image captured when the temporary occlusions appear contain large occlusions that do not appear in other LR images captured at a different time. Furthermore, temporary occlusions may appear at different locations in different LR images. For example, a leaf moving in the wind may appear at one location in one LR image but a different location in another LR image captured using the same camera at a different time. Permanent occlusions are artifacts that are always present regardless of time. An example of this is large artifacts caused by dirt on the lens of a camera. Unless the dirt is cleaned off of the lens, all image captured using this camera will exhibit the same dirt artifacts. It is necessary to deal with both types of occlusions to reduce the effect of large scale artifacts on the reconstructed HR image.

Fig. 2. Example of large scale artifacts. Left: large dirt and dust artifacts; Right: objects that move in and out of frame

Current super-resolution methods do not account for the presence of such large scale artifacts. Therefore, such techniques blindly make use of all information from the LR images whether it is erroneous information or not. Therefore, any erroneous information due to large scale artifacts are used in the reconstruction of the HR image, resulting in significant loss in perceptual quality. The goal of the proposed algorithm is prevent such erroneous information from contributing to the final HR image.

B. Problem Partitioning

The first step in the proposed algorithm is to partition the full multi-frame super-resolution problem into a number of smaller multi-frame super-resolution problems. This serves two main purposes:

1) Reduce computational cost, and
2) Allow for local artifact detection.

Let us first discuss the computational cost reduction gained from partitioning the full super-resolution problem into a number of smaller super-resolution problems. Let there exist n $[M \times N]$ LR images and the desired resolution enhancement is R. The multi-frame super-resolution problem in Section II can be rewritten in matrix-vector form as:

$$\left(\underline{I}_{\mathrm{LR},j}\right)_{:} = \mathrm{H}_j \left(\underline{I}_{\mathrm{HR}}\right)_{:} + \underline{e}_j, 1 \leq j \leq n \tag{4}$$

where $\left(\underline{I}_{\mathrm{LR},j}\right)_{:}$ is a $[MN \times 1]$ vector representing the j^{th} LR image lexicographically ordered, $\left(\underline{I}_{\mathrm{HR}}\right)_{:}$ is a $[(R^2MN) \times 1]$ vector representing the HR image lexicographically ordered, H_j is a $[(MN) \times (R^2MN)]$ matrix representing representing the degradation model, and $\underline{e}_j$ a $[MN \times 1]$ vector representing the additive noise in the j^{th} image. Combining the n equations (one for each LR image) as expressed by (4) yields the following:

$$\begin{bmatrix} \left(\underline{I}_{\mathrm{LR},1}\right)_{:} \\ \left(\underline{I}_{\mathrm{LR},2}\right)_{:} \\ \vdots \\ \left(\underline{I}_{\mathrm{LR},j}\right)_{:} \\ \vdots \\ \left(\underline{I}_{\mathrm{LR},n}\right)_{:} \end{bmatrix} = \begin{bmatrix} \mathrm{H}_1 \\ \mathrm{H}_2 \\ \vdots \\ \mathrm{H_j} \\ \vdots \\ \mathrm{H_n} \end{bmatrix} \left(\underline{I}_{\mathrm{HR}}\right)_{:} + \begin{bmatrix} \underline{e}_1 \\ \underline{e}_2 \\ \vdots \\ \underline{e}_j \\ \vdots \\ \underline{e}_n \end{bmatrix} \tag{5}$$

This can be expressed in a simplified form as:

$$\overline{\underline{I}}_{\mathrm{LR}} = \overline{\mathrm{H}} \left(\underline{I}_{\mathrm{HR}}\right) + \overline{\underline{e}} \tag{6}$$

As stated earlier, the super-resolution problem is ill-posed in most practical situations, since they involve underdetermined systems. To make the problem well-posed, a prior model can be introduced. The problem posed (6) can be formulated as a regularized optimization problem. This can be expressed as follows:

$$\hat{\underline{I}}_{\mathrm{HR}} = \arg\min \left\{ \left\| \begin{bmatrix} \overline{\underline{I}}_{\mathrm{LR}} \\ 0 \end{bmatrix} - \begin{bmatrix} \overline{\mathrm{H}} \\ -\sqrt{\lambda}\mathrm{L} \end{bmatrix} \hat{\underline{I}}_{\mathrm{HR}} \right\| \right\} \tag{7}$$

where L is the constraints matrix and λ is the relaxation values that controls the degree of approximation of the system. This regularized optimization problem can be solved efficiently using the LSQR algorithm [20], a fast iterative linear systems solver that is designed for large least-squares problems. One of the biggest issues is that, even when a efficient solver such as LSQR is used, it is still very computationally expensive to solve the full multi-frame super-resolution problem

as a whole. In the case of n $M \times N$ LR images and a resolution enhancement factor of R, the estimated cost of LSQR per iteration is $2(R^2MN)(MN(n+1))$ multiplications per iteration. Suppose that the problem is now partitioned into K^2 sub-problems, with each problem representing a $[RM/KRN/K]$ section of the final HR image. The estimated computational cost of performing LSQR on this sub-problem becomes $(1/K^4)2(R^2MN)(MN(n+1))$ multiplications per iteration. Since K^2 sub-problems need to be solved, the computational cost of solving the problem in this manner is $(1/K^2)$ of solving the problem as a whole. Furthermore, the memory requirements for solving each sub-problem is approximately $(1/K^4)$ the size of solving the problem as a whole. Therefore, significant computational and memory performance gains can be achieved by partitioning the problem into smaller sub-problems.

The second purpose of partitioning the full multi-frame super-resolution problem into smaller sub-problems is to allow for the detection of large-scale artifacts in a local manner. As mentioned earlier, the general characteristics of large scale artifacts are not known as they can vary greatly from one LR image to another. This makes it difficult to detect large-scale artifacts globally based on specific characteristics or properties. By partitioning the global problem into smaller local problems, large-scale artifacts can be identified more easily within a smaller sample window based on local characteristics. For example, a large dust artifact may account for 5% of the total image content and thus appear to be relatively insignificant quantitatively if taken on a global scope. However, this large dust artifact becomes quantitatively significant within a local window that covers 6% of the total image content.

In the proposed algorithm, the full super-resolution problem is divided into q smaller super-resolution problems that represent a partition in the HR image that overlaps parts of its neighboring partitions. Once the individual sub-problems are solved, they are recombined to form the final HR image. While the size and the overlap amount of the partitions are set depending on the situation at hand, it is intuitive that the overlap amount should be kept reasonable low to reduce computational cost while remaining large enough to reduce blocking artifacts that result due to discontinuities between partitions. The size of the partitions should also be small enough such that the presence of a large scale artifact has a significant effect on the local characteristics but large enough such that it is not overly sensitive to small variations.

C. Artifact Detection

Once the full super-resolution problem has been partitioned into smaller sub-problems, local artifact detection is performed on each sub-section. As stated earlier, the general characteristics of large scale artifacts are not known as they can vary greatly from one LR image to another. This makes it difficult to detect large-scale artifacts based on specific properties. For example, a circular-shaped dust artifact may appear to obstruct the scene at one location in the first LR image (captured by the first camera) while a different dust artifact with an irregular shape may appear at a different location in the second LR image (captured by a second camera). However, since multiple LR images are captured of the same scene, the fact that different large scale artifacts act differently from one LR image to another can be exploited to isolate these artifacts from true image content.

While large scale artifacts may appear with different properties at random locations, one general assumption that can be made is that the probability that the same artifact appears at the same location in all the LR images is relatively low. In the case of permanent occlusions, a particular artifact may appear in all LR images produced by one camera but not in the LR images proposed by the other cameras. In the case of temporary occlusions, a specific particular artifact may appear in LR images produced within a certain time frame but not in LR images produced at another time frame. Therefore, large scale artifacts can be classified as all information that is not largely consistent with the information contained in the majority of LR images used to reconstruct the HR images. Otherwise, if the same large scale artifact appears at the same location in all LR images, no additional information can be obtained about that occluded region in any case since the no "correct" information was captured there in the first place.

One method of isolating information that is inconsistent with the majority of LR images is to determine the dissimilarity between the information contained within one LR image with the information contained in all other LR images. If the dissimilarity between the information from one LR image and that in all other LR images is sufficiently high, it can be said that the information is inconsistent with the majority of the LR images and therefore is classified as a large scale artifact. In the proposed algorithm, the following artifact detection method was performed for each sub-problem:

1) For each image partition P_i, calculate the RMSE between the partition and every other image partition P_j as follows:

$$\mathrm{RMSE}\left(P_i, P_j\right) = \sqrt{E\left(\left(P_i - P_j\right)^2\right)} \tag{8}$$

where $E()$ is the expected value.

2) The dissimilarity metric R between P_i and all other partitions is computed as:

$$\mathrm{R}\left(P_i\right) = \frac{1}{n-1}\sum_{i \neq j} \mathrm{RMSE}\left(P_i, P_j\right) \tag{9}$$

where n is the number of image partitions.

3) The image partition P_i is classified as a large scale artifact if the following condition is satisfied:

$$\mathrm{R}\left(P_i\right) > t \tag{10}$$

where t is a threshold value that separates between non-artifacts and artifacts. The value of t can be adjusted based on the distinctiveness of the large scale artifacts. The more distinctive the artifacts are from the actual image content, the greater the value of t can be set to avoid false positives.

D. Adaptive Regularized Optimization

Based on the large scale artifact detection results from Section III-C, each sub-problem is adaptively constructed by discarding image partitions that are classified as large scale artifacts and retaining a subset of non-artifact partitions. The resultant adaptive regularized optimization problem formulation for each sub-problem can be expressed as:

$$\underline{\hat{I}}_{\mathrm{HR},k} = \arg\min \left\{ \left\| \begin{bmatrix} \overline{\underline{I}}_{\mathrm{LR},k} \\ 0 \end{bmatrix} - \begin{bmatrix} \overline{\mathrm{H}}_k \\ -\sqrt{\lambda}_k \mathrm{L}_k \end{bmatrix} \underline{\hat{I}}_{\mathrm{HR},k} \right\| \right\} \tag{11}$$

where L_k, λ_k are the constraints matrix and relaxation values for the k^{th} sub-problem, and $\overline{\underline{I}}_{\mathrm{LR},k}$ and $\overline{\mathrm{H}}_k$ represent the subset of non-artifact partitions and its corresponding degradation operators respectively for the k^{th} sub-problem. As such, the problem formulation will be adaptively adjusted based on the number of non-artifact partitions in each sub-problem. What this does is effectively prevent erroneous information caused by large scale artifacts from affecting the reconstructed HR image by removing them from the problem altogether.

So far, the selection of λ values have not been discussed. The λ values control the degree of approximation of the system. Large λ values improve the conditioning of the regularized optimization problem but in a poor approximation of the original problem. Therefore, the selection of λ values become a tradeoff between smoother estimations (large values) and closer resemblance to the original information obtained from the LR images (small values). In the proposed algorithm, the relaxation values are adaptively adjusted based on the edge characteristics derived from the LR images. The human vision system is highly sensitive to blurring in edge regions but less sensitive to noise in edge regions than smooth regions. Therefore, pixels that lie in edge regions should be assigned a lower relaxation value to preserve edge detail and thus improve perceptual quality. For test purposes, pixels in edge regions are assigned a λ value of 0.2 while those in non-edge regions are assigned a λ value of 1.

IV. Testing Methods

To investigate the effectiveness of the proposed algorithm, three test sets consisting of sixteen 8-bit grayscale LR images were used. A brief description of the test sets is provided below.

1) **TEST1**: Set of LR images generated from an image of a jeep. The LR images are contaminated by large dirt artifacts.
2) **TEST2**: Set of LR images generated from an image of an altar in a church. The LR images are contaminated by large dirt artifacts.
3) **TEST3**: Set of LR images generated from images of a highway. The LR images are contaminated by moving cars.

Each LR image was synthetically generated from the original HR image(s) by applying translational motion, blur, and decimation by a factor of four for each dimension. In the case of TEST1 and TEST2, the LR images are then contaminated by randomly generated large dirt artifacts. In the case of TEST1 and TEST2, two base HR images are used to generated the LR images, one containing no cars and one containing cars. The LR images are then generated from either of the two HR images. The proposed algorithm was then used to reconstruct a HR image at four times the resolution of the LR image using only 9 of the 16 LR images. To provide a quantitative measure of quality for the reconstructed HR image, the Peak Signal-to-Noise Ratio (PSNR) was calculated between the reconstructed HR image and the original HR image.

V. Experimental Results

A summary of the PSNR between the original image and the images produced with and without the proposed artifact reduction method is presented in Table I. It can be observed that HR images produced with the proposed artifact reduction method shows noticeable PSNR gains for all test sets when compared to not using the proposed artifact reduction method. These results demonstrate the effectiveness of the proposed method at reducing the effect of large scale artifacts on the reconstructed HR image. Examples of the resultant HR images using the proposed method are shown in Fig. 3, Fig. 4, and Fig. 5. It can be observed that the perceptual quality for the reconstructed HR images produced using the proposed method are noticeably improved when compared to those constructed without using the proposed method.

TABLE I
PSNR for Test Sets

Test Set	PSNR		PSNR Gain
	Without Artifact Reduction	With Artifact Reduction	
TEST1	29.6607	31.2243	+1.5636
TEST2	27.4590	28.0660	+0.6070
TEST3	28.0811	28.8895	+0.8084

VI. Conclusions and Future Work

In this paper, we have introduced a novel adaptive approach to large scale artifact reduction in multi-frame image super-resolution. By utilizing information from different LR images, prominent large scale artifacts are detected and adaptively prevented from contributing to the construction of the HR image. Experimental results showed high perceptual quality can be achieved using the proposed method to reduce the effects of large scale artifacts. It is our belief that the proposed method can be used successfully for the purpose of multi-frame super-resolution in situations where prominent large scale artifacts exist in the LR images.

Acknowledgment

This research has been sponsored in part by the Natural Sciences and Engineering Research Council of Canada.

Fig. 3. Super-resolution results of TEST 1; From Left to Right: a) bilinear interpolated from a LR image, b) without artifact reduction, c) with artifact reduction

Fig. 4. Super-resolution results of TEST 2; From Left to Right: a) bilinear interpolated from a LR image, b) without artifact reduction, c) with artifact reduction

Fig. 5. Super-resolution results of TEST 3; From Left to Right: a) bilinear interpolated from a LR image, b) without artifact reduction, c) with artifact reduction

REFERENCES

[1] T. Taxt and R. Jirik, "Superresolution of ultrasound images using the first and second harmonic signal Ultrasonics," *IEEE Transactions on Ferroelectrics and Frequency Control*, vol. 51, no. 2, pp. 163 - 175, 2004.

[2] G. Clement, J. Huttunen, and K. Hynynen, "Superresolution ultrasound imaging using back-projected reconstruction," *The Journal of the Acoustical Society of America*, vol. 118, no. 6, pp. 3953-3960, 2005.

[3] H. Li and D. Doermann, "Superresolution-based enhancement of text in digital video," *Proceedings on the International Conference on Pattern Recognition*, vol. 1, pp. 847-850, 2000.

[4] Y. Altunbasak, A. Patti, and R. Mersereau, "Super-resolution still and video reconstruction from MPEG-coded video," *IEEE Transactions on Circuits and Systems for Video Technology*, vol. 12, no. 4, pp. 217-226, 2002.

[5] K. Donaldson and G. Myers, "Bayesian super-resolution of text in video with a text-specific bimodal prior," *Proceedings of the IEEE Computer Society Conference on Computer Vision and Pattern Recognition*, vol. 1, pp. 1188-1195, 2005.

[6] C. Rubert, L. Fonseca, and L. Velho, "Learning based super-resolution Using YUV model for remote sensing images," *Proceedings of WTD-CGPI*, 2005.

[7] H. Tao, X. Tang, J. Liu, and J. Tian, "Superresolution remote sensing image processing algorithm based on wavelet transform and interpolation," *Proceedings of SPIE: Image Processing and Pattern Recognition in Remote Sensing*, vol. 4898, pp. 259-263, 2003.

[8] W. Freeman, T. Jones, E. Pasztor, "Example-based super-resolution," *IEEE Computer Graphics and Applications*, vol. 1, no. 2, pp. 56-65, 2002.

[9] A. Zomet and S. Peleg, "Efficient super-resolution and applications to mosaics," *Proceedings of International Conference on Pattern Recognition*, vol. 1, pp. 579-583, 2000.

[10] N. Nguyen, P. Milanfar, and G. Golub, "A Computationally Efficient Superresolution Image Reconstruction Algorithm," *IEEE Transactions on Image Processing*, vol. 10, no. 4, pp. 573-583, 2001.

[11] F. Cortijo, S. Villena, R. Molina, and A. Katsaggelos, "Bayesian super-resolution of text image sequences from low resolution observations," *Proceedings on International Symposium on Signal Processing and Its Applications*, vol. 1, pp. 421-424, 2003.

[12] D. Capel and A. Zisserman, "Super-resolution enhancement of text image sequences," *Proceedings on International Conference on Pattern Recognition*, vol. 1, pp. 600605, 2000.

[13] K. Sauer and J. Allebach, "Iterative reconstruction of band-limited images from nonuniformly spaced samples," *IEEE Transactions on Circuits and Systems*, vol. 34, no. 12, pp. 1497-1506, 1987.

[14] A. Patti and Y. Altunbasak, "Artifact reduction for set theoretic super resolution image reconstructions with edge adaptive constraints and higher-order interpolants," *IEEE Trans. Image Processing*, vol. 10, no. 1, pp. 179-186, 2001.

[15] M. Irani and S. Peleg, "Improving resolution by image registration," *Proceedings of CVGIP: Graphical Models and Image Processing*, vol. 53, no. 3, pp. 231239, 1991.

[16] M. Elad and A. Feuer, "Restoration of a single superresolution image from several blurred, noisy, and undersampled measured images," *IEEE Transactions on Image Processing*, vol. 6, no. 12, pp. 1646-1658, 1997.

[17] A. Lettington and Q. Hong, "Ringing artifact reduction for Poisson MAP superresolution algorithms," *IEEE Signal Processing Letters*, vol. 2, no. 5, pp. 83-84, 1995.

[18] C. Miravet and F. Rodriguez, "A hybrid MLP-PNN architecture for fast image superresolution," *Lecture Notes in Computer Science*, vol. 2714, pp. 401-408, 2003.

[19] Z. Xu and X. Zhu, "Super-Resolution Reconstruction of Compressed Video Based on Adaptive Quantization Constraint Set," *International Conference on Innovative Computing, Information and Control*, vol. 1, pp. 281-284, 2006.

[20] C. Paige and M. Saunders, "LSQR: an algorithm for sparse linear equations and sparse least squares," *ACM Transactions On Mathematical Software*, vol. 8, no. 1, pp. 43-71, 1982.